Michigan State University

National Superconducting Cyclotron Laboratory

MASS DEPENDENCE OF DIRECTED COLLECTIVE FLOW

M.J. HUANG, R.C. LEMMON, F. DAFFIN, W. G. LYNCH, C. SCHWARZ, M. B. TSANG, C. WILLIAMS, P. DANIELEWICZ, K. HAGLIN, W. BAUER, N. CARLIN, R.J. CHARITY, R.T. DE SOUZA, C. K. GELBKE, W.C. HSI, G.J. KUNDE, M-C. LEMAIRE, M.A. LISA, U. LYNEN, G.F. PEASLEE, J. POCHODZALLA, H. SANN, L.G. SOBOTKA, S.R. SOUZA, and W. TRAUTMANN

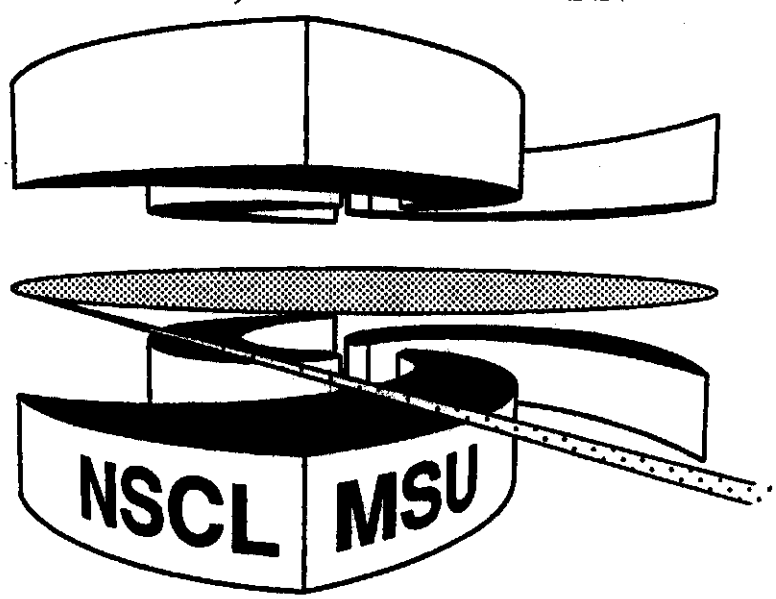

MSUCL-1024 **APRIL 1996**

Mass Dependence of Directed Collective Flow

M.J. Huang[a], R.C. Lemmon", F. Daffin[a], W.G. Lynch", C. Schwarz[ad], M.B. Tsang[a], C. Williams", P. Danielewicz", K. Haglin[a], W. Bauer', N. Carlin[f], R.J. Charity", R.T. de Souza[e], C.K. Gelbke", W.C. Hsi[ae], G.J. Kunde[ad], M-C. Lemaire[b], M.A. Lisa", U. Lynen[d], G.F. Peaslee[a], J. Pochodzalla[d], H. Sann[d], L.G. Sobotka[c], S.R. Souza[b], and W. Trautmann[d]

[a] *NSCL and Department of Physics and Astronomy, Michigan State University, East Lansing, MI 48824, USA.* [b] *Laboratoire National SATURNE, CEN Saclay, 91191 Gif-sur-Yvette Cedex, France.* [c] *Department of Chemistry, Washington University, St. Louis, MO 63130, USA.* [d] *Gesellschaft für Schwerionenforschung, D-6100 Darmstadt 11, Germany.* [e] *IUCF and Department of Chemistry,* Indiana *University, Bloomington, IN 47405, USA.* [f] *Instituto de Fisica, Universidade de São Paulo, CEP 01498, São Paulo, Brazil.*

Abstract

Sidewards directed fragment flow has been extracted for $^{84}Kr+^{197}Au$ collisions at E/A=200 MeV, using techniques that are free of reaction plane dispersion. The fragment flow per nucleon increases with mass, following a thermal- or coalescence-like behavior, and attains approximately constant limiting values at $4 \leq A \leq 12$. Comparisons of the impact parameter dependences of the measured coalescence-invariant proton flow to Boltzmann-Uehling-Uhlenbeck calculations clearly favor a momentum dependent nuclear mean field.

25.75.+r, 25.70.Pq

The determination of the equation of state (EOS) of nuclear matter is an important objective of nuclear physics. Information about the equation of state can be extracted from the collective flow of nuclear matter deflected sidewards from the hot and dense region formed by the overlap of projectile and target nuclei [1,2]. This flow reflects the interplay of collective and random motions. For a thermalized system, the random motions of emitted fragments are dictated by the thermal energy, which is independent of mass. Contributions to the fragment energy due to collective motion, on the other hand, increase linearly with mass, making the flow more easily observed for heavier fragments [3,4].

Measurements of light charged particle (p,d,t,α) flow confirm that transverse collective flow increases with mass [3]. Limited studies for Z>2 confirm that intermediate mass fragments exhibit stronger flow effects than light charged particles [4], but a systematic understanding of the dependence of collective flow upon fragment mass is lacking. Such information is essential for quantitative flow extraction at incident energies E/A$\leq$250 MeV, where fragments remove much of the total mass [5,6]. In this letter we provide the first quantitative examination of the mass dependence of collective flow which includes intermediate mass fragments up to Z=6. We explore these effects with the mass-asymmetric ^{84}Kr+ ^{197}Au system which allows clear distinctions between different parameterizations of the nuclear EOS.

In the experiment, 5 mg/cm^2 thick ^{197}Au targets were bombarded with 200A MeV ^{84}Kr beams of the Laboratoire National SATURNE at Saclay. The emitted charged particles were detected with 276 low-threshold plastic-scintillator-CsI(Tl) phoswich detectors of the combined Miniball/ Wall array [7], which covered 90% of 4π in solid angle. Unit charge resolution beyond Z$\sim$12 was routinely achieved for particles which stopped in the CsI(Tl) scintillators. Ball detectors at backward angles, θ_{lab}= 25°-160°, incorporated 4 mg/cm^2 scintillator foils and 2 cm thick CsI(Tl) crystals and had particle identification (PID) thresholds of E_{th}/A $\sim$2

(4) MeV for Z=3 (10) particles, respectively. Wall detectors at forward angles, θ_{lab}=5.4°-25°, incorporated 8 mg/cm^2 foils and 3 cm thick CsI(Tl) crystals and had PID thresholds of 4 (6) MeV for Z=3 (10) particles, respectively. Flow analyses were performed within an energy gate of E/A = 20-75 MeV which took the minimum energy for ^{3}He and α separation and the range for energetic protons in the Miniball detectors into account. An impact parameter scale was constructed from the total detected charged particle multiplicity and normalized via cross section measurements [5]. Further details about the experiment can be found in Ref. [5].

The in-plane component of the directed flow is usually extracted by techniques [8], wherein the momenta of detected particles are projected onto an experimentally determined reaction plane . At incident energies of E/A$\approx$ 200 MeV, techniques for locating this reaction plane utilize asymmetries in the emission patterns of particles which originate from their deflection from the compressed overlap region between projectile and target nuclei. Experimentally extracted reaction planes generally fluctuate about the true reaction plane for each event [9], however, introducing uncertainties in the extracted transverse momenta. Corrections for this reaction plane dispersion may be applied, but have uncertainties that become especially large when the flow is small [10].

To avoid such uncertainties, another technique has been proposed which involves constructing appropriate mean products of the measured momenta [11]. In this technique, the inner product $p_\nu^\perp(y_\nu) \cdot p_\mu^\perp(y_\mu)$ between the transverse momentum $p_\nu^\perp(y_\nu)$ of a particle of type ν at rapidity y_ν and the transverse momentum $p_\mu^\perp(y_\mu)$ of a particle of type μ at rapidity y_μ is averaged over the transverse momenta of the two particles. The random fluctuations of the transverse momenta about the collective mean values then average to zero leaving only the collective mean values. Choosing a coordinate system in which the non-vanishing mean collective transverse momenta lie along the x axis, this average inner product

becomes [11]:

$$\langle p_\nu^\perp(y_\nu) \cdot p_\mu^\perp(y_\mu)\rangle \simeq \langle p_\nu^x(y_\nu)\rangle\langle p_\nu^x(y_\nu)\rangle. \quad (1)$$

Momentum conservation gives rise to further correlations between particle transverse momenta, modifying Eq. (1) to read [11]:

$$\langle p_\nu^\perp(y_\nu) \cdot p_\mu^\perp(y_\mu)\rangle \simeq \langle p_\nu^x(y_\nu)\rangle\langle p_\nu^x(y_\nu)\rangle - \alpha\langle p_\nu^{\perp^2}(y_\nu)\rangle\langle p_\mu^{\perp^2}(y_\mu)\rangle \quad (2)$$

where $\alpha^{-1} \simeq \langle \sum_\mu p_\mu^{\perp^2}\rangle$ [11] and the sum runs over all emitted particles. (Since the experimental detection efficiency in the present experiment is less than one, the value for α^{-1} used in Eq. (2) was obtained by rescaling the experimental value for α^{-1} by the ratio of the total to the detected mass [12].) Final state interactions and apparatus non-uniformities can influence the extraction of the mean transverse momenta [11]; corrections have been made for these effects following ref. [11] but make little difference to the final results presented here.

Mean two-fragment inner products $\langle p_\nu^\perp(y_\nu) \cdot p_\mu^\perp(y_\mu)\rangle$ are then constructed for each possible pair of particle types with $1 \leq Z_1, Z_2 \leq 6$ and selected bins of normalized rapidity, $y_n = y_{cm}/y_{beam}$. Eq. (2) is then solved by matrix diagonalization to obtain initial values for $\langle p_\nu^x(y_\nu)\rangle$ in the different rapidity bins [11]. Final values for $\langle p_\nu^x(y_\nu)\rangle$ are obtained by a least squares minimization procedure in which the $\langle p_\nu^x(y_\nu)\rangle$ on the r.h.s. of Eq. (2) are varied from their initial values so as to accurately satisfy Eq. (2). This procedure permitted an assessment of the uncertainties in the values for $\langle p_\nu^x(y_\nu)\rangle$.

Data were analyzed for two impact parameter gates: $1 \leq b \leq 3$ fm and $4 \leq b \leq 6$ fm. Within these gates, analyses were performed for particles with $-0.2 \leq y_n \equiv y/y_{beam} \leq 0.2$ in the center of momentum (c.m.) frame where deficiencies in the Miniball acceptance cause few distortions. The suitability of this criterion is illustrated for alpha particles in Fig. 1(a) where thermal model simulations for the

mean transverse momenta of are shown with (filtered) and without (unfiltered) corrections for the experimental acceptance; this criterion is similarly suitable for the other analyzed particles as well. (Further details of these simulations are given below.) Measured mean transverse momenta per nucleon $\langle p^x/A \rangle$, shown in Fig. 1(b) for protons and Be fragments at $4 \leq b \leq 6$ fm, reveal enhanced transverse momenta for heavier particles, consistent with trends observed in previous studies [3,4]. Near $y_n = 0$, the data in Fig. 1(b) are linear and well characterized by the collective flow, $F = d\langle p^x/A \rangle / dy_n$, which can be easily extracted via a linear least-squares fit near mid-rapidity. (Note that $\langle p_x/A \rangle$ does not cross zero at $y_n = 0$ for asymmetric systems.)

The flow per nucleon, $d\langle p^x/A \rangle / dy_n$, is shown as a function of fragment mass in Fig. 2 for the two impact parameter gates. Not surprisingly, the flow per nucleon is larger for the more peripheral gate. The flow increases monotonically with mass for $Z \leq 2$, consistent with previous measurements [3,4,13]. For fragments with $Z > 2$, however, the flow is approximately independent of mass. This is the first time that the mass dependence of directed flow has been observed for intermediate mass fragments with sufficient statistics to examine this dependence in detail.

To examine the interplay between collective and thermal motion more quantitatively, we have simulated the velocity distributions of the fragments with a thermal expression of the form

$$P(\mathbf{v}) = \int d\mathbf{v} \mathcal{F}(\mathbf{v}_{coll}) \mathcal{G}(\mathbf{v}_{th}) \delta(\mathbf{v} - \mathbf{v}_{coll} - \mathbf{v}_{th}). \qquad (3)$$

Here, we assume a collective velocity distribution of Gaussian form $\mathcal{F}(\mathbf{v}_{coll}) \propto exp(-\sum_i [\mathbf{v}^i_{coll}]^2 / 2\sigma_i^2)$ with three independent principal axes to approximate the situation before breakup. We then assume that the momenta of the produced particles obtain additional random velocity components according to the distribution $\mathcal{G}(\mathbf{v}_{th}) \propto exp(-A\mathbf{v}^2_{th}/2T)$, where A is the fragment mass number and T

is a temperature parameter. The principal axes of the collective velocity distribution are rotated by the flow angle, θ_F; σ_3 characterizes the distribution along the flow axis and σ_1 and σ_2 characterizes the other widths in and perpendicular to the reaction plane, respectively. These widths were adjusted to reproduce the measured rapidity and transverse energy distributions. The solid line in Fig. 2, for calculations assuming $\sigma_1 = 0.1c, \sigma_2 = 0.1c, \sigma_3 = 0.16c, \theta_F = 40°$, and $T = 45$ MeV, reproduces the main experimental trends. While this parameterization is not unique, the observed constancy of the heavy fragment flow can only be reproduced if it is primarily governed by the collective velocity distribution. The flow for light particles is then reduced relative to that for heavy fragments due to thermal mixing between the collective velocity distributions at positive and negative rapidities in the c.m. system.

Since coalescence and thermodynamic models make equivalent predictions in the limit of local thermal equilibrium [14], the agreement between the measured and calculated mass dependence can be regarded as a partial justification for the utilization of cluster production mechanisms [15] that have similarities to the coalescence approximation. For comparisons to the proton flow predicted by transport models such as the Boltzmann-Uehling-Uhlenbeck (BUU) equation, we have taken advantage of this observation to construct an effective proton flow

$$F_{eff} = \sum Z_i Y_i F_i / \sum Z_i Y_i, \tag{4}$$

where the Z_i, Y_i, and F_i are the charge, yield, and flow values for the various particle species. In Fig. 3 the experimental effective proton flow is plotted against impact parameter as the solid points. The width of the horizontal bars represents the relevant impact parameter bin. Note that the effective proton flow exceeds the measured proton flow, as expected for the coalescence model which creates clusters and depletes free proton flux in densely occupied regions in phase space, where collective phenomena are most strongly manifested.

To test the sensitivity of this measurement to the transport parameters, BUU calculations have been performed for various parameterizations of the mean field potential and including a nucleon-nucleon cross section which has been parameterized to describe measured nucleon-nucleon scattering data [16]. These calculations are shown in Fig. 3 for a soft (K=200 MeV) mean field (**SM** - small triangles) and a hard (K=386 MeV) mean field (**HM** - large triangles) with a momentum dependence consistent with non-locality effects observed in nucleon-nucleus potential scattering [17]. Calculations with a soft mean field (**S** - open squares) and a hard mean field (**H** - open circles) without momentum dependence are also shown. All calculations have been impact parameter averaged and filtered by the experimental acceptance.

The qualitative trends of the data are much better described by momentum dependent mean fields. The degeneracy between calculations with soft momentum dependent and hard momentum independent mean fields, observed for symmetric Nb+Nb or La+La [18–20] systems, is broken for this mass asymmetric system, consistent with the observations of ref. [20]. The sensitivity to the compressibility parameter K is slight, however. Consistent with the systematics of the disappearance of collective flow [21] and with microscopic calculations of the in-medium corrections to the nucleon-nucleon cross section [22], improved agreement between the momentum dependent calculations and the data can be obtained by a 20% density dependent reduction of the in-medium nucleon-nucleon cross section of the form $\sigma_{NN} = (1 - 0.2\frac{\rho}{\rho_o})\sigma_{free}$ [21], This is illustrated by the solid points in the Fig. 3 for a soft momentum dependent mean field (**SM** $(\mathbf{0.8}\sigma_{free})$).

In summary, we have measured the mass dependence of sidewards directed collective flow for the system ^{84}Kr+^{197}Au at an incident energy of 200 MeV/A, where fragments carry a significant fraction of the mass and the collective flow. The flow for light fragments has a linear mass dependence, but is nearly indepen-

dent of mass for intermediate mass fragments with Z>2. The mass dependence is essentially reproduced by model calculations which superimpose a thermal velocity distribution upon a collective velocity distribution. These calculation suggests that the flow of heavy fragments is governed essentially by the collective velocity distribution. Comparisons to BUU calculations demonstrate a clear preference for a momentum dependent mean field and offer support for a 20% density dependent reduction in the nucleon-nucleon cross-section from the value in free space.

This work is supported by the National Science Foundation under Grants No. PHY-90-15255, PHY-92-14992, and PHY-94-03666 and the U.S. Department of Energy under Contract No. DE-FG02-87ER-40316. W.G.L and L.G.S. acknowledge the receipt of U.S. Presidential Young Investigator Awards. W.B. acknowledges support from the U.S. NSF PFF program. N. Carlin and S.R. Souza acknowledge partial support by the CNPq, Brazil. We gratefully acknowledge the support and hospitality extended to us during our experiment at the LNS.

REFERENCES

[1] H.H. Gutbrod, A.M. Poskanzer and H.G. Ritter, Rep. Prog. Phys., **52,** 1267 (1989) and refs. therein.

[2] H. Stöcker and W. Greiner, Phys. Rep., **137,** 277 (1986) and refs. therein.

[3] M.D. Partlan *et al.*, Phys. Rev. Lett. **75**, 2100 (1995).

[4] K.G.R. Doss *et al.*, Phys. Rev. Lett. **59**, 2720 (1986).

[5] G. Peaslee *et al.*, Phys. Rev. C **49**, R2271 (1994).

[6] M. B. Tsang et al., Phys. Rev. Lett. **71**, 1502 (1993).

[7] R.T. de Souza et al, Nucl. Instr. Meth. A 295, 109 (1990); The Miniwall, a granular extension of the Miniball to forward angles, uses the readout technology of D.W. Stracener et al, Nucl. Inst. Meth. A 294, 485 (1990).

[8] P. Danielewicz and G. Odyniec, Phys. Lett. **157B**, 146 (1985).

[9] Here, the reaction plane is defined to be perpendicular to the total angular momentum.

[10] J.P. Sullivan and J. Péter, Nucl. Phys. **A540**, 275 (1992).

[11] P. Danielewicz *et al.*, Phys. Rev. C **38**, 120 (1988).

[12] This ratio was of order 0.3, but varied with impact parameter [5]. Recoil corrections are small.

[13] S. Wang *et al.*, Phys. Rev. Lett. **74**, 2646 (1995).

[14] L.P. Csernai and J.I. Kapusta, Phys. Rep. **131,** 223 (1986) and refs. therein.

[15] P. Danielewicz and G.F. Bertsch, Nucl. Phys. **A533**, 712 (1991).

[16] D. Klakow, G. Welke, and W. Bauer, Phys. Rev. **C48**, 1982 (1993).

[17] C. Gale et. al., Phys. Rev. **C41**, 1545 (1990).

[18] C. Gale et al., Phys. Rev. **C35**, 1666 (1987).

[19] J. Aichelin et al., Phys. Rev. Lett. **58**, 1926 (1987).

[20] Q. Pan and P. Danielewicz, Phys. Rev. Lett. **70**, 2062, 3523 (1993).

[21] G.D. Westfall et al., Phys. Rev. Lett. **71**, 1986 (1993).

[22] T. Alm, Nucl. Phys. **A587**, 815 (1995).

FIG. 1.(a) Simulations for the transverse momenta of α particles with the thermal model of Eq. 3. Open and filled circles depict calculations with the model before and after corrections for the experimental acceptance have been applied. (b) Mean transverse momenta measured for p and Be fragments at 4<b<6 fm.

FIG. 2. The mass dependence of the collective sidewards flow per nucleon in the reaction plane, $d\langle p_x/A\rangle/dy_n$ for the two impact parameter gates used in the analysis. Here we assume A=2Z for A> 4, where mass identification was not achieved. The solid line shows a calculation with the thermal model of Eq.3.

FIG. 3. The solid square points with horizontal error bars depict the measured effective proton flow. Also shown are the corresponding BUU calculations for the following parameter sets: **H** - hard EOS without momentum dependence (open circles), **S** - soft EOS without momentum dependence (open squares), **HM** - hard EOS with momentum dependence (large triangles), **SM** - soft EOS with momentum dependence (small triangles). **SM** ($\mathbf{0.8\sigma_{free}}$) - soft EOS with momentum dependence and a 20% reduction in the nucleon-nucleon cross-section (solid circles). The theoretical error bars are purely statistical.

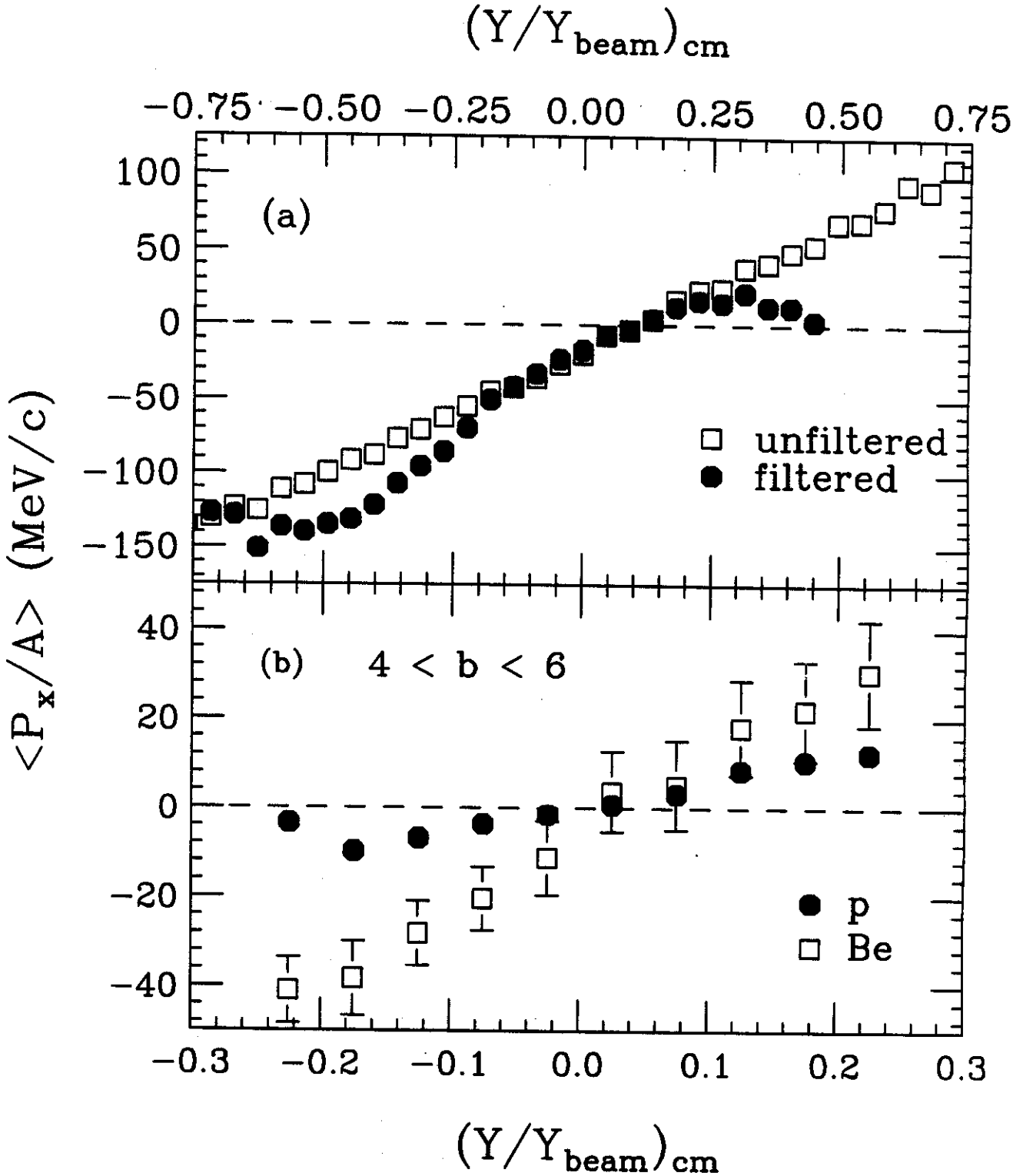
$(Y/Y_{beam})_{cm}$
−0.75 −0.50 −0.25 0.00 0.25 0.50 0.75
100
50
0
−50
−100
−150
(a)
unfiltered
filtered
$\langle P_x/A \rangle$ (MeV/c)
40
20
0
−20
−40
(b) 4 < b < 6
p
Be
−0.3 −0.2 −0.1 0.0 0.1 0.2 0.3
$(Y/Y_{beam})_{cm}$

Figure 1.

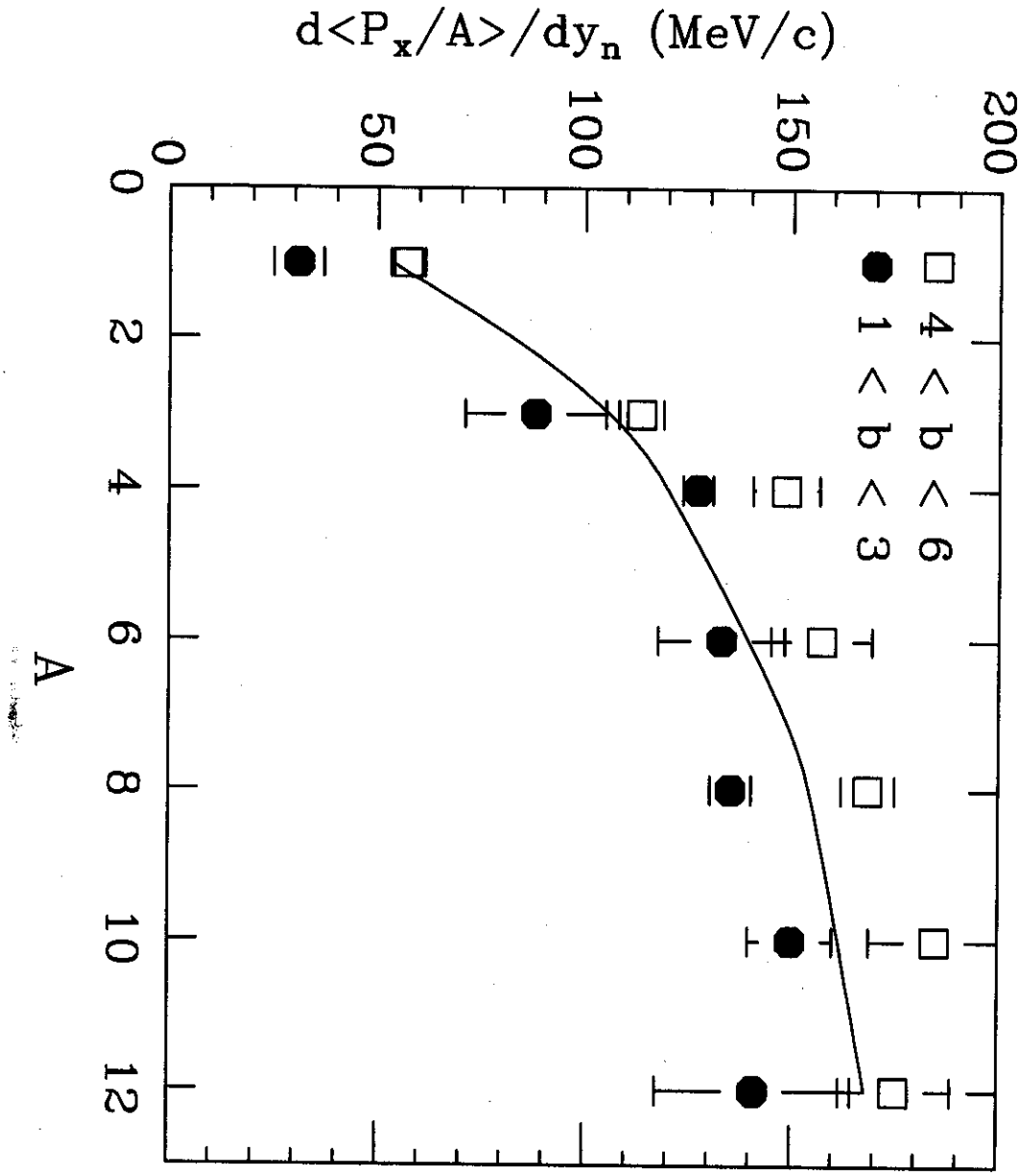

Figure 2.

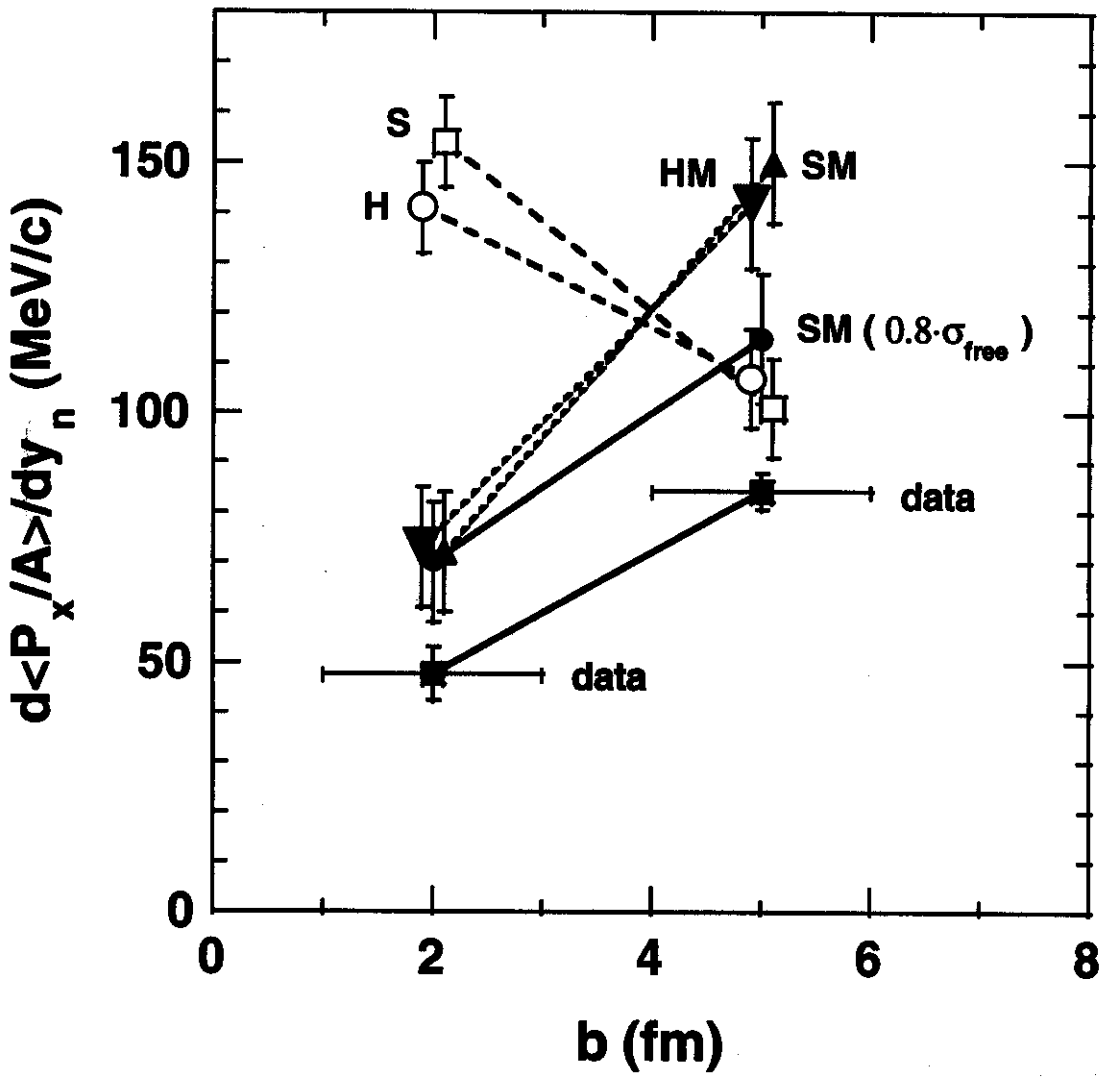
S
H
HM
SM
SM (0.8·σfree)
data
data
150
100
50
0
0
2
4
6
8
d<Px /A>/dyn (MeV/c)
b (fm)

Figure 3.